

MARTENSITIC TRANSITION IN SINGLE-CRYSTALLINE α -GeO₂ AT COMPRESSION

V.V.Brazhkin, E.V.Tat'yanin, A.G.Lyapin, S.V.Popova, O.B.Tsiok,
D.V.Balitskii*

Institute for High Pressure Physics RAS, 142092 Troitsk, Moscow reg., Russia

* *M.V.Lomonosov Moscow State University, 119899 Moscow, Russia*

Submitted 28 February 2000

We present the structural study of single crystalline quartz-like α -GeO₂ compressed to pressures up to 12 GPa and subsequently quenched to ambient conditions. The transition to a new crystalline phase with a distorted rutile structure, occurring in the pressure interval 8 to 12 GPa, was established. The structure of the new phase was identified from X-ray and electron diffraction data as $P2_1/c$ monoclinic. Electron transmission and scanning microscopy provide direct evidence of the martensitic (or displacive) nature of the transition, indicating, in particular, the lamellar morphology and crystallographic orientation relation between initial α -quartz and final new monoclinic phases. Upon heating, the new monoclinic phase transforms to the rutile-type structure with a similar (and similarly oriented) oxygen structure motif. Finally, we discuss the difference in high-pressure behavior of single-crystalline and polycrystalline samples, transforming to the new crystalline and amorphous phases, respectively.

PACS: 61.50.Ks, 64.60.My, 81.30.Kf, 81.40.Vw

Polymorphism of silica SiO₂ is of great interest for geophysics, Earth and planetary sciences, and glass technology. Germanium dioxide GeO₂ is the closest structural and polymorphic analog of silica. In particular, the α -quartz modification of GeO₂ is structurally very similar to α -quartz SiO₂ under pressure (they have a close intertetrahedral angle) [1]. From this point of view the study of GeO₂ under pressure could extend our knowledge about tetrahedrally networked crystalline and glassy compounds, including silicates and germanates.

α -Quartz SiO₂ undergoes gradual pressure-induced amorphization from 15 to 30 GPa with an intermediate crystalline-to-crystalline transition (quartz I-II) at 21 GPa [2–4]. Amorphous silica samples quenched to normal conditions display unusual properties such as anisotropy and “memory” effects [5], that may be described theoretically [6]. In nonhydrostatic conditions α -quartz transforms to a mixture of amorphous and new crystalline phases [7], based probably on the edge-sharing SiO₆ octahedra structures. Another low-pressure polymorph of silica, cristobalite, transforms to a stishovite-like phase under quasi-hydrostatic compression [8]. A variety of theoretically proposed silica structures with highly coordinated Si atoms ($Z > 4$) [9–12] suggests a complicated picture of metastable high-pressure polymorphism in silica.

The α -GeO₂ phase transforms in the pressure interval 6 ÷ 8 GPa to the amorphous state with the rutile-like short-range order structure, the coordination of Ge atoms being changed from four- to sixfold at high pressure [13–17]. The low pressure of amorphization for germania glass gives the opportunity to study large samples under pressure. Another motivation of the current work is to study the influence of sample morphology and nonhydrostaticity on the transformation type. There are indications that the type of high-pressure transformation in AlPO₄ can depend on the initial crystal size [18]. Un-

fortunately, the α -quartz modification of GeO_2 is metastable at normal conditions [19], and only polycrystalline specimens with a small grain size have been used for high pressure investigations to date. Here we present the structural study of the sample recovered at normal conditions after both hydrostatic and quasi-hydrostatic compression of large single crystals of α - GeO_2 . This type study is of special interest for understanding more general aspects of the solid state amorphization phenomenon [20–22].

Experimental. Large α - GeO_2 single crystals (several millimeters in size) were prepared using a novel hydrothermal technique described in detail in Refs.[23, 24]. The pieces used in our experiments were $4 \times 4 \times 1$ mm platelets with the crystallographic c axis perpendicular to the largest sides. A high structural quality of α - GeO_2 single crystals allowed us to study earlier the elastic constants of quartz-like GeO_2 by Brillouin spectroscopy [25].

The high pressure up to 12 GPa was generated in the toroid-type chamber [26] with the 4:1 methanol:ethanol mixture and polycrystalline NaCl as the hydrostatic or quasi-hydrostatic pressure transmitting media, respectively. The compression and subsequent decompression of samples were carried out at room temperature with the pressure change rate ~ 0.2 GPa/min. The structure of recovered samples was studied by both electron (the JEM-100C transmission electron microscope – TEM) and X-ray (the Debye-Scherrer method) diffraction techniques. The morphology of samples was studied by electron scanning microscopy (Leica S430 and Stereoscan MK-2). The density of samples was measured by the picnometric method. The MOM-C Derivatograph (Hungary) was used for the annealing of samples at ambient pressure.

Results and discussion. In our experiments we applied pressure to both, polycrystalline (with small grain size on the order of a micron or less) and single-crystalline α - GeO_2 samples. The polycrystalline samples recovered from pressure higher than 8 GPa were completely disordered in accordance with the published data on the pressure-induced amorphization of α - GeO_2 . Quite a different picture was revealed for single-crystalline α - GeO_2 . The transition to a new crystalline GeO_2 polymorph takes place instead of that to an amorphous phase. The transition occurs in a wide pressure range starting at 7 to 7.5 GPa and finishing at 11.5 to 12 GPa. At intermediate pressures we observed a mixture of the new high-pressure phase and the initial quartz-like polymorph. The transition was found to follow the almost identical scenario both in hydrostatic and quasi-hydrostatic conditions.

X-ray diffraction data revealed that the new high-pressure GeO_2 phase had the structure fairly similar to that of rutile-type GeO_2 , but with a more complicated X-ray diffraction pattern (see Table). In particular, the strong reflections of the new phase with the d -space 0.240, 0.218, and 0.210 nm coincide or are very close to the (101), (200), and (111) rutile reflections, respectively. On the other hand, the strong reflections with d -spacing 0.290, 0.261, and 0.230 nm are absent in the diffraction pattern of the rutile phase.

Electron diffraction on a single crystallite of the recovered material provides more comprehensive structural data (Table and Figure). Among the known and theoretically proposed GeO_2 (SiO_2) structures, the 3×2 monoclinic structure with the $P2_1/c$ space group [11] was established to agree best with the diffraction from the new phase (see Table). This structure consists of 3×2 kinked edge-sharing GeO_6 octahedral chains and can be regarded as a distorted hexagonal close-packed (hcp) array of oxygen ions with one-half of the available octahedral interstices occupied by Ge ions in the specific

zigzag (3×2) order [11]. The indexing of diffraction patterns in accordance with this consideration leads to the lattice parameters: $a = 0.815$ nm, $b = 0.436$ nm, $c = 0.535$ nm, $\alpha = \gamma = 90^\circ$, and $\beta = 118^\circ$.

Experimental d -spacing and relative intensities (only for X-ray data) for the new GeO_2 phase, compared with the d -spacing of the GeO_2 rutile and 3×2 monoclinic $P2_1/c$ structures

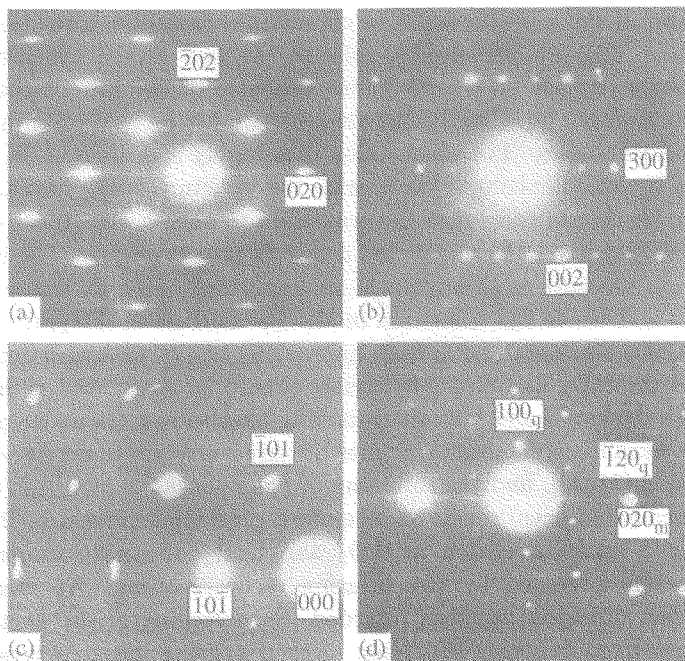
New phase			Rutile*		$P2_1/c$ -type**	
TEM	X-ray		hkl	d_{hkl} (nm)	hkl	d_{hkl} (nm)
d (nm)	d (nm)	I/I_{max} (%)				
0.473						
0.387	0.393	5			11 $\bar{1}$	0.335
0.335	0.336	20			011	0.320
0.321			110	0.311		
	0.312	10			21 $\bar{1}$	0.289
0.289	0.290	80			10 $\bar{2}$	0.264
0.264					111	0.263
0.263					20 $\bar{2}$	0.262
0.262	0.261	60			300	0.240
0.240	0.240	100	101	0.240	002	0.236
0.236	0.235	40			30 $\bar{2}$	0.231
0.231	0.230	50			31 $\bar{1}$	0.230
	0.218	30	200	0.220	020	0.218
0.218	0.218	30	111	0.210	310	0.210
0.210	0.210				211	0.209
	0.208	20			012	0.208
0.208	0.207				102	0.199
0.199			210	0.197		
	0.193				40 $\bar{2}$	0.193
0.193					12 $\bar{2}$	0.168
0.168	0.168	10			22 $\bar{2}$	0.168
	0.165	15			202	0.165
0.165	0.164		211	0.162		
	0.161				320	0.161
0.161					50 $\bar{2}$	0.161
	0.159	80			022	0.160
0.159	0.159				32 $\bar{2}$	0.159
	0.150	10	220	0.155		
0.150	0.151		002	0.143	51 $\bar{1}$	0.150
	0.139	40			411	0.139
0.139	0.138				302	0.139
0.138	0.135	10			60 $\bar{2}$	0.136
0.136	0.135					

*Lattice parameters are $a = 0.4396$ nm and $c = 0.2863$ nm.

**Lattice parameters are $a = 0.815$ nm, $b = 0.436$ nm, $c = 0.535$ nm, $\alpha = \gamma = 90^\circ$, and $\beta = 118^\circ$.

The new phase annealing at normal pressure displayed its metastability, since it gradually transformed to rutile GeO_2 in the temperature interval 200 to 500 °C with a small exothermal effect. When the new phase transforms to the stable rutile modification during annealing, the reflection $d = 0.240$ nm from the corresponding part of the sample is the same before and after the transition (Fig.b and c). This reflection corresponds to the (101) rutile lattice planes. The transition of the 3×2 monoclinic structure to the rutile one may be interpreted as a reordering of Ge ions in the distorted hcp oxygen array,

when the oxygen structural motive is retained. The atomic packings of the (101) planes of the rutile structure and the (100) planes of the new phase are similar in this case. The crystallographic density of the 3×2 monoclinic phase (6.22 g/cm^3) is slightly less than that of the rutile GeO_2 (6.28 g/cm^3), the experimentally measured value is ($6.1 \pm 0.05 \text{ g/cm}^3$).



Electron diffraction patterns: a, b – from the monoclinic phase of GeO_2 for 101 and 010 zones (reciprocal lattice planes), respectively; c – from rutile phase (010 zone of rutile structure) obtained upon annealing of the monoclinic phase; and d – from the partly transformed area revealing both initial α -quartz (001 zone) and new monoclinic modifications (the reflections for $\bar{1}07$ and 001 zones can be observed transitionally and crystallographically to one another (reflections of the monoclinic phase are marked by index “m”). The patterns b and c are obtained from the same crystallite before and after annealing

The electron diffraction from the areas containing both initial α -quartz and the final new phase in incompletely transformed samples (Fig.d) provides direct evidence of the martensitic (or displacive) mechanism of the pressure-induced crystalline-crystalline transition in α - GeO_2 . The lamellar morphology of the recovered samples, visualized by scanning electron microscopy, also proves this conclusion. We have established the following crystallographic orientational relations between the initial quartz-like and new phases, if the latter is indentified as the 3×2 monoclinic $P2_1/c$ structure: $(100)^{\alpha\text{-quartz}}$ nearly $\parallel (100)^{\text{monoclinic}}$ and $(\bar{1}20)^{\alpha\text{-quartz}}$ nearly $\parallel (010)^{\text{monoclinic}}$. There are three possible orientations for the produced phase with respect to the initial α - GeO_2 crystal, because α -quartz has three planes equivalent to the (100). The observed surface morphology pictures for the recovered samples support this statement, the three lamellar sets being relatively located at an angle of 60° to each other.

More careful examination of the experimental data showed that the agreement between experimental data and the new phase identification as a 3×2 monoclinic structure was still not ideal. First, in the experimental diffraction spectra (Table) there are some

reflections forbidden for the $P2_1/c$ structure; second, there is no good agreement between the experimental and the calculated reflection intensities (this point is not considered in detail here). These observations indicate that the new GeO_2 phase, probably based on the 3×2 monoclinic structure, contains large amount of the (010) packing defects of the monoclinic lattice.

The mechanism of the pressure-induced crystalline-crystalline transition demands a special discussion. The crystallographic relation, as well as the specifically oriented lamellar morphology provide an unambiguous evidence of the atomic-cooperative displacive transformation mode. Clearly, the transition must be governed in this case by dynamic softening principles. The observation of a highly coordinated SiO_2 phase (obtained under non-hydrostatic compression) with the structure fairly similar to the 3×2 monoclinic phase [7, 11] indicates that the transition to such a structure is an ordinary phenomenon for the tetrahedrally networked α -quartz structure type. The hydrostaticity degree for the high-pressure environment is an important dynamic factor affecting the phonon spectrum and hence the transition mode. In contrast to SiO_2 , the distorted rutile structure of GeO_2 was obtained in both hydrostatic and quasi-hydrostatic conditions. The difference in the SiO_2 and GeO_2 behaviors should be associated with specific features of the lattice dynamics and the corresponding phonon spectra under pressure. One should note that dynamic softening principles are used now for understanding the solid state amorphization [21, 22], and the softening of open-packed structures (in particular, tetrahedrally coordinated ones) seems to be quite a general phenomenon [22].

The α -quartz-to-rutile transition in SiO_2 and GeO_2 occurring under pressure at high temperatures is governed by the diffusion reconstruction. At room and lower temperatures, when diffusion becomes retarded, the softening of the particular modes in the phonon spectrum becomes a driving force triggering the structural reconstruction. This gives a key for understanding the difference between the crystalline-to-crystalline, crystalline-to-amorphous, and amorphous-to-amorphous transformations in quartz-like GeO_2 . The coordination transformation in amorphous GeO_2 under pressure [14, 15, 27, 28] is determined by a wide spectrum of activation energies for local coordination reconstructions [28], the property which seems to be inherent in the disordered GeO_2 network because of the dispersion of bond lengths and bond-bond angles, as well as the topological disorder in the arrangement of GeO_4 tetrahedra. In the opposite case of single-crystalline α - GeO_2 , the transition results in a coherent cooperative atomic movement. Polycrystalline α - GeO_2 is an intermediate case. When the average grain size is small enough the scenario of coherent displacive transition is destroyed because the dispersion of stresses in individual crystallites and a large portion of defective atomic sites at grain boundaries cause the disorder. These factors seem to create a great variety of topologically different displacive soft modes for the coordination reconstruction and lead to the formation of the topologically disordered GeO_2 structure, although, the different displacive modes may have rather similar geometrical reasons for softening (for example, like twisting of SiO_4 tetrahedra in the α -quartz near the pressure of amorphization transformation [29]). One should note that in the amorphous samples thus obtained the structural disorder varies from really amorphous nanoregions to those with a high degree of the rutile type crystallinity [14]. The difference between the pressure intervals for the solid state amorphization and the crystalline-to-crystalline transition in materials with the same atomic structure but different morphology, emphasizes the dynamic difference in the ways of transformation. The properties of high-pressure amorphous samples ob-

tained from starting amorphous and polycrystalline quartz-like GeO_2 are also different [13, 14].

Further structural and dynamic investigation of single $\alpha\text{-GeO}_2$ crystals under pressure, including the Raman and Brillouin spectroscopy studies, are expected to provide additional understanding of the high-pressure behavior of tetrahedrally networked GeO_2 and SiO_2 polymorphs. Computer simulation will be very suitable for the identification of real displacive modes during the transition.

We are grateful to S.C.Bayliss, A.V.Sapelkin, M.Grimsditch, and A.Polian for stimulating discussions, to I.Fletcher (Faculty of Applied Science, De Montfort University, Leicester, LE1 9BH, England) for assistance in the scanning microscopy study, and to N.F.Borovikov and L.A.Ivanov for assistance in the optic microscopy study. This work was supported in part by the Russian Foundation for Basic Research (project #98-02-16325) and by the program "Integratsiya" (grant #250).

1. L.Levien, C.T.Prewitt, and D.J.Weidner, *Am. Mineral.* **65**, 920 (1980).
2. R.J.Hemley, A.P.Jephcoat, H.K.Mao et al. *Nature* **334**, 52 (1988).
3. K.J.Kingma, C.Meade, R.J.Hemley et al., *Science* **259**, 666 (1993).
4. K.J.Kingma, R.J.Hemley, H.-K.Mao, and D.R.Veblen, *Phys. Rev. Lett.* **70**, 3927 (1993).
5. L.E.McNeil and M.Grimsditch, *Phys. Rev. Lett.* **68**, 83 (1992).
6. J.S.Tse and D.D.Klug, *Phys. Rev. Lett.* **70**, 174 (1993).
7. K.J.Kingma, H.-K.Mao, and R.J.Hemley, *High Press. Res.* **14**, 363 (1996).
8. M.Yamakata and T.Yagi, *Rev. High Pressure Sci. Technol.* **7**, 107 (1998).
9. B.B.Karki, M.C.Warren, L.Stixrude et al., *Phys. Rev.* **B55**, 3465 (1997).
10. J.Badro, D.M.Teter, R.T.Downs et al., *Phys. Rev.* **B56**, 5797 (1997).
11. D.M.Teter, R.J.Hemley, G.Kresse, and J.Hafner, *Phys. Rev. Lett.* **80**, 2145 (1998).
12. R.M.Wentzcovitch, C.D.Silva, J.R.Chelikowsky, and N.Binggeli, *Phys. Rev. Lett.* **80**, 2149 (1998).
13. T.Yamanaka, T.Shibata, S.Kawasaki, and S.Kume, in *High-Pressure Research: Application to Earth and Planetary Sciences*, Eds. Y.Syono and H.Manghnani, American Geophysical Union, Washington, D.C., 1992, p.493.
14. G.H.Wolf, S.Wang, C.A.Herbst et al., in *High-Pressure Research: Application to Earth and Planetary Sciences*, Eds Y.Syono and H.Manghnani, American Geophysical Union, Washington, D.C., 1992, p.503.
15. J.P.Itie, A.Polian, G.Calas et al., *Phys. Rev. Lett.* **63**, 398 (1989).
16. N.Suresh, G.Jyoti, S.C.Gupta et al., *J. Appl. Phys.* **76**, 1530 (1994).
17. S.Kawasaki, *J. Mater. Sci. Lett.* **15**, 1860 (1996).
18. P.Gillet, J.Badro, B.Varrel, and P.F.McMillan, *Phys. Rev.* **B51**, 11262 (1995).
19. E.Yu.Tonkov, *High Pressure Phase Transformations*, A Handbook 1-2, Gorgon and Breach, Philadelphia, 1992.
20. E.G.Ponyatovsky and O.I.Barcalov, *Mat. Sci. Rep.* **8**, 1471 (1992).
21. V.V.Brazhkin and A.G.Lyapin, *High Press. Res.* **15**, 9 (1996).
22. A.G.Lyapin and V.V.Brazhkin, *Phys. Rev.* **B54**, 12036 (1996).
23. D.V.Balitskii, Y.Pushchanskii, and V.S.Imlitsky, in *Abstracts of the 11-th Intern. Conf. on Crystal Growth*, The Hague, Netherlands, 1995, p.573.
24. V.S.Balitsii, D.V.Balitskii, D.Yu.Putsharovskii et al., in *Experimental and Theoretical Modelling of the Processes of Mineral Formation*, Eds. V.A.Zharikov and V.V.Fed'kin, Moscow, Nauka, 1998, p.498.
25. M.Grimsditch, A.Polian, V.Brazhkin, and D.Balitskii, *J. Appl. Phys.* **83**, 3018 (1998).
26. L.G.Khvostantsev, L.F.Vereshchagin, and A.P.Novikov, *High Temp.-High Press.* **9**, 637 (1977).
27. K.H.Smith, E.Shero, A.Chizmeshya, and G.H.Wolf, *J. Chem. Phys.* **102**, 6851 (1995).
28. O.B.Tsiok, V.V.Brazhkin, A.G.Lyapin, and L.G.Khvostantsev, *Phys. Rev. Lett.* **80**, 999 (1998).
29. С.В.Горяинов, Н.Н.Овсяук, *Письма в ЖЭТФ* **69**, 431 (1999).